



**University of
Zurich**^{UZH}

**Zurich Open Repository and
Archive**

University of Zurich
University Library
Strickhofstrasse 39
CH-8057 Zurich
www.zora.uzh.ch

Year: 2019

High-density ECoG improves the detection of high frequency oscillations that predict seizure outcome

Boran, Ece ; Ramantani, Georgia ; Krayenbühl, Niklaus ; Schreiber, Maxine ; König, Kristina ; Fedele, Tommaso ; Sarnthein, Johannes

Abstract: OBJECTIVES: Residual fast ripples (FR) in the intraoperative ECoG are highly specific predictors of postsurgical seizure recurrence. However, a FR is generated by a small patch of cortical tissue. Spatial sampling with standard electrodes may thus miss clinically relevant information.

DOI: <https://doi.org/10.1016/j.clinph.2019.07.008>

Posted at the Zurich Open Repository and Archive, University of Zurich

ZORA URL: <https://doi.org/10.5167/uzh-173172>

Journal Article

Accepted Version

Originally published at:

Boran, Ece; Ramantani, Georgia; Krayenbühl, Niklaus; Schreiber, Maxine; König, Kristina; Fedele, Tommaso; Sarnthein, Johannes (2019). High-density ECoG improves the detection of high frequency oscillations that predict seizure outcome. *Clinical Neurophysiology*, 130(10):1882-1888.

DOI: <https://doi.org/10.1016/j.clinph.2019.07.008>

High-density ECoG improves the detection of high frequency oscillations that predict seizure outcome.

Ece Boran¹, Georgia Ramantani², Niklaus Krayenbühl¹, Maxine Schreiber¹, Kristina König³, Tommaso Fedele⁴, Johannes Sarnthein^{1,5,*}

¹ Klinik für Neurochirurgie, UniversitätsSpital und Universität Zürich, Switzerland

² Neuropädiatrie, Universitäts-Kinderspital Zürich, Switzerland

³ Schweizerisches Epilepsie-Zentrum, Zürich, Switzerland

⁴ National Research University Higher School of Economics, Moscow, Russian Federation

⁵ Zentrum für Neurowissenschaften Zürich, ETH Zürich, Switzerland

* Corresponding author at: Klinik für Neurochirurgie, UniversitätsSpital Zürich, 8091 Zürich, Switzerland.

E-mail address: johannes.sarnthein@usz.ch (J. Sarnthein).

Keywords: epilepsy surgery; intraoperative recording; Fast Ripple; resection area; seizure outcome

Highlights:

1) High-density (hd) ECoG increases the number of Fast Ripples (FR) detected during epilepsy surgery.

2) hd-ECoG improves the prediction of seizure outcome after resective epilepsy surgery.

3) hd-ECoG may advance seizure freedom after epilepsy surgery.

Abstract

Objectives: Residual fast ripples (FR) in the intraoperative ECoG are highly specific predictors of postsurgical seizure recurrence. However, a FR is generated by a small patch of cortical tissue. Spatial sampling with standard electrodes may thus miss clinically relevant information.

Methods: We analyzed FR rates in the intraoperative ECoG of 22 patients that underwent resective epilepsy surgery. We used standard electrodes with 10 mm inter-contact spacing (standard ECoG) in 14 surgeries and high-density grid electrodes with 5 mm spacing (hd-ECoG) in 8 surgeries. We detected FR using a previously validated automatic detector.

Results: Postoperative seizure freedom was achieved in 14/22 (64%) cases. Across all 42 ECoG recordings, FR rates were higher for hd-ECoG than for standard ECoG. In the 14 seizure free patients (ILAE 1), no residual FR were detected (specificity = 100%). In the 8 patients with seizure recurrence (ILAE > 1), residual FR were detected in 1/7 standard ECoG and 1/1 hd-ECoG (Accuracy $ACC_{\text{standard ECoG}} = 57\%$, CI [29% 82%], $ACC_{\text{hd-ECoG}} = 100\%$, CI [63% 100%]).

Conclusion: Denser spatial sampling by hd-ECoG improved FR detection compared to standard ECoG.

Significance: Hd-ECoG may advance seizure freedom after epilepsy surgery.

1 Introduction

Epilepsy surgery is the treatment of choice in selected patients with drug-resistant focal epilepsy (Ryvlin et al., 2014). The efficacy of surgical treatment regarding seizure alleviation depends on the complete resection of the epileptogenic brain tissue (Jette et al., 2014). Intraoperative ECoG recordings serve the detection of epileptic discharges, i.e. spikes or spike-waves, generated by the epileptogenic brain tissue, against healthy cortical areas. However, several studies have showed that interictal epileptic discharges lack a stable correlation with disease activity (Grewal et al., 2019, Zijlmans et al., 2009a, 2009b), questioning their reliability as a biomarker to monitor treatment response.

In recent years, interictal High Frequency Oscillations (HFO, > 80 Hz), recorded in epileptogenic brain tissue, have been identified as a reliable biomarker for the delineation of the epileptogenic zone (Fedele et al., 2019, Frauscher et al., 2017, Jiruska et al., 2017, Thomschewski et al., 2019, Zijlmans et al., 2017). HFO are classified according to their spectral range in ripples (80-250 Hz) and fast ripples (FR, 250-500 Hz). Intraoperative electrocorticography (ECoG) and invasive EEG studies have specifically pointed at FR as reliable predictors of seizure outcome in epilepsy surgery, since the incomplete resection of electrode locations with FR has been shown to result in seizure recurrence in the individual patient (Fedele et al., 2017a, Fedele et al., 2017b, van 't Klooster et al., 2015a, van 't Klooster et al., 2015b, Wu et al., 2010).

Currently, it is a major challenge to detect FR during surgery and to use their localization in real time to accordingly tailor a resection. FR are generated by a small patch of cortical tissue, i.e. they are spatially highly localized and have a low amplitude (Burnos et al., 2016, Jiruska et al., 2017, von Ellenrieder et al., 2014). Standard subdural ECoG electrodes with 10 mm spacing between contacts may be suboptimal for detecting FR, resulting in false outcome prediction. Using electrodes with closer contact spacing (high-density, hd) increases the spatial resolution but requires smaller contacts. Since smaller contacts have higher impedance and thereby lower signal-to-noise ratio, the use of hd electrodes may not necessarily enhance FR detection (Zijlmans et al., 2017). Thus, defining the optimal spatial resolution for recording clinically relevant FR remains a challenge.

In this study, we compare FR detection between standard ECoG electrodes with 10 mm spacing between contacts and high-density (hd) ECoG electrodes with 5 mm spacing. As a primary endpoint, we show that hd-ECoG improves the detection of clinically relevant FR. As a secondary endpoint, we illustrate how residual FR predict seizure outcome in the individual patient.

2 Methods

2.1 Patients

We retrospectively included pediatric and adult patients who underwent resective epilepsy surgery in our institution, guided by intraoperative ECoG, between July 2015 and April 2018. We included all consecutive patients with post-resection ECoG and follow-up-duration of ≥ 12 months. We excluded patients with palliative surgery. Postsurgical seizure outcome was determined according to the ILAE scale and consecutively classified into two categories: seizure freedom (ILAE 1) and seizure recurrence (ILAE 2-5).

2.2 Anesthesia management

According to our standard protocol for neurosurgical interventions, anesthesia was induced with intravenous application of propofol (1.5–2 mg/kg) and fentanyl (2–3 $\mu\text{g/kg}$). Intratracheal intubation was facilitated by atracurium (0.5 mg/kg). Anesthesia was maintained with propofol (5–10 mg/kg/h) and remifentanyl (0.1–2 $\mu\text{g/kg/min}$). Twenty minutes before ECoG recording, propofol was ceased and anesthesia was sustained with sevoflurane ($\text{MAC} < 0.5$).

2.3 ECoG recordings

Intraoperative ECoG was recorded using either standard subdural grid and strip electrodes (standard ECoG, **Figure 1a**, AdTech Medical) or high-density subdural grid electrodes (hd-ECoG, **Figure 1e**, AdTech Medical). The standard ECoG electrodes had a contact exposure diameter of 5 mm and an inter-electrode distance of 10 mm. The hd-ECoG electrodes had a contact exposure diameter of 2.3 mm and an inter-electrode distance of 5 mm. We used a needle electrode placed in the dura as electrical reference. We collected ECoG data from all patients with a Nicolet recording device (Nicolet® CSeries amplifier: Natus Medical Incorporated, 16-bit ADC, Pleasanton, PA, USA; sampling rate 2 kHz, 1-800 Hz passband). All ECoG data was re-referenced to a bipolar montage. Intervals with visible artifacts and

channels affected by continuous interference or not recording from brain tissue were excluded from further analysis.

The placement of subdural electrodes for intraoperative ECoG was guided solely by the clinical question. Only interictal epileptiform discharges (and not HFO) were considered for the intraoperative delineation of the epileptogenic zone and thus for tailoring the resection. Before the resection, we recorded ECoG from 1-3 contiguous locations over the area to be resected and its margins. After the resection, we again recorded from 1-3 contiguous locations at the resection margins, depending on the clinical question and the accessibility of specific brain regions through the craniotomy. ECoG electrode localization was determined and carefully documented by the neurosurgeon and neurologist in charge of the patient.

2.4 HFO analysis

For HFO detection, we used an automated detector previously validated against seizure outcome in intraoperative ECoG (Fedele et al., 2017b, Fedele et al., 2019, Fedele et al., 2016). The automated detector had three stages. In Stage I, the amplitude threshold (Th_{amp}) is set in the HFO spectral domain. Time intervals with high Stockwell entropy (low oscillatory activity) define the background activity. A low Th_{amp} indicates a low noise level in the signal, i.e. good signal quality. Events exceeding Th_{amp} are marked as events of interest (EoI). In Stage II, we selected all EoI that exhibited a high frequency peak isolated from low frequency activity in the time-frequency space (Burnos et al., 2014).

The number of EoI was further reduced in Stage III. Here we eliminate artifacts with multichannel spread, as opposed to FR, which are spatially confined in a small patch of cortical tissue (Burnos et al., 2016, von Ellenrieder et al., 2014). EoI on channels that exhibited a correlation coefficient > 0.8 in the FR band with any other channel at a distance > 10 mm were rejected (Fedele et al., 2016). This methodology rejects EoI with immediate spread but does not reject EoI that are recorded with a delay across multiple channels, therefore “travelling HFO” are not rejected. Note that in standard ECoG, an EoI spreading over two adjacent bipolar channels was not eliminated, since the distance between these channels equals 10 mm and does not exceed 10 mm.

This prospective definition of a clinically relevant HFO has been previously shown to predict seizure outcome with high accuracy (Fedele et al., 2017b, Fedele et al., 2016). Following these steps of automated HFO detection, we performed visual validation. For each event, an observer inspected the signal in a 0.3 s window around the event in the full band and filtered in the FR band.

For our primary endpoint, we computed the FR rate for each recording and selected the pre- and post-resection recordings with the highest FR rate (**Table 1**). For the selected recordings, we computed the maximum FR amplitude for the channel with the highest FR rate. We then compared the distributions of FR rates and FR amplitudes across electrode types (**Figure 2**). We chose to compare the maximum FR rate between pre- and post- resection ECoG recordings and performed no statistical tests, since the presence of even a single channel with residual FR has been shown to predict seizure recurrence (Fedele et al., 2017b, Fedele et al., 2016, van 't Klooster et al., 2015a, van 't Klooster et al., 2015b, van 't Klooster et al., 2017).

2.5 Prediction of seizure outcome using residual FR

For our secondary endpoint, i.e. to quantify the predictive value of FR with respect to seizure outcome in each patient, we determined whether residual FR were detected in post-resection ECoG. Residual FR were those detected in the last post-resection ECoG recording, indicating that the FR-generating tissue had not been fully resected. FR rates $\geq 1/\text{min}$ indicated the presence of residual FR (Fedele et al., 2017b, Fedele et al., 2016).

We divided the patients into four groups. True Positive (TP): residual FR, seizure recurrence (ILAE >1) correctly predicted; True Negative (TN): no residual FR, seizure freedom (ILAE 1) correctly predicted; False Positive (FP): residual FR, seizure freedom falsely predicted; False Negative (FN): no residual FR, seizure recurrence falsely predicted. The positive predictive value was calculated as $\text{PPV} = \text{TP}/(\text{TP} + \text{FP})$, negative predictive value as $\text{NPV} = \text{TN}/(\text{TN} + \text{FN})$, sensitivity as $\text{Sens} = \text{TP}/(\text{TP} + \text{FN})$, specificity as $\text{Spec} = \text{TN}/(\text{TN} + \text{FP})$, and accuracy as $\text{ACC} = (\text{TP} + \text{TN})/(\text{TP} + \text{TN} + \text{FP} + \text{FN})$.

2.6 Statistics

We compared the distributions of FR rates and amplitudes between standard ECoG and hd-ECoG using the Wilcoxon rank sum test. Statistical significance was defined for $p < 0.05$. We used the binomial method to estimate 95% confidence intervals (CI).

2.7 Ethical considerations

The collection of personal patient data and their analysis were approved and performed conform to the guidelines and regulations of the local research ethics committee (Kantonale Ethikkommission KEK-ZH-Nr. PB-2017-00094). The collection of patients' written informed consent was waived. All data used in this study will be made publicly available upon acceptance of the manuscript.

3 Results

3.1 Patients

Of 25 patients that underwent resective epilepsy surgery guided by intraoperative ECoG, 22 patients (10 male, 13 pediatric) met the inclusion criteria. We excluded three patients due to: 1) palliative surgery, 2) multifocal cortical dysplasia with insufficient ECoG coverage and 3) no post-resection ECoG recordings in one patient each, resulting in 22 cases in our study (**Table 1**).

3.2 Surgery

Of 22 resections, 8 were temporal, 5 frontal, 6 parietal and 3 occipital. Histopathology revealed FCD in 9, tumors with glial components in 7, cavernoma in 2, Sturge-Weber syndrome in 3 cases and hippocampal sclerosis in 1 case (**Table 1**).

3.3 Postsurgical outcome

Fourteen of 22 (64%) resections led to seizure freedom (ILAE 1), including 7 of 14 guided by standard ECoG and 7 of 8 guided by hd-ECoG (**Table 1**). The median (IQR) postsurgical follow-up period was 30 (18-35) months across all cases and did not differ significantly between patients with seizure freedom and seizure recurrence (median 29 vs. 33 months). The follow-up period of seizure-free patients did not differ significantly between resections guided by standard ECoG and hd-ECoG (median 31 vs. 24 months).

3.4 Intraoperative ECoG

We recorded both pre- and post-resection ECoG in 12 of 14 standard ECoG cases. In 2 cases, we only recorded post-resection ECoG. We included 110 bipolar channels in the analysis, with a median (IQR) of 4 (3-5) channels per recording. We excluded 64 bipolar channels because of artifacts, with a median (IQR) of 1 (0-4) channel per recording.

We recorded both pre- and post-resection ECoG in all eight hd-ECoG cases. We included 356 bipolar channels in the analysis (23 (20-24) channels per recording). We excluded 88 bipolar channels because of artifacts (6 (4-8) channels per recording). Hd-ECoG recordings had a higher number of channels available for analysis ($p = 5.6 \times 10^{-8}$, Wilcoxon rank sum test).

This resulted in a total of 42 pre- and post-resection recordings in our study. We report the recording duration for each patient in **Table 1**.

For standard ECoG, the total duration of recordings was 95 minutes (3 (3-4) minutes per patient). For hd-ECoG, the total duration of recordings was 58 minutes (with 3 (2-4) minutes per patient). The duration of recordings for standard ECoG and hd-ECoG did not differ. Hence, the advantage of hd-ECoG over standard ECoG does not stem from a difference in recording duration.

3.5 Hd-ECoG improved FR detection

Figure 1 shows examples of FR detected with standard ECoG and hd-ECoG in pre-resection recordings. Patient 13 underwent a right parietal resection with standard ECoG (**Figure 1a-d**). No FR were detected in post-resection ECoG, but the patient suffered from recurrent seizures (ILAE 5), and was therefore classified as False Negative (FN). Patient 1 underwent a left parietal resection with hd-ECoG (**Figure 1e-h**). No FR were detected in post-resection ECoG and the patient was seizure free (ILAE 1) for > 2.5 years, and was therefore classified as True Negative (TN).

For the primary endpoint of our study, we compared standard ECoG and hd-ECoG recordings with respect to FR detection. The distribution of maximum FR amplitude and maximum FR rate over recordings for both electrode types is presented in **Figure 2**. The maximum event amplitude for the channel with the maximum FR rate seemed higher for hd-ECoG (**Figure 2b**, $15.29 \pm 13.65 \mu\text{V}$, $\text{Th}_{\text{amp}} = 1.30 \pm 0.39 \mu\text{V}$) than for standard ECoG ($10.74 \pm 12.85 \mu\text{V}$, $\text{Th}_{\text{amp}} = 1.94 \pm 0.88 \mu\text{V}$) but this did not reach statistical significance ($p = 0.4559$, Wilcoxon rank sum test). As our main result, the maximum event rate was significantly higher for hd-ECoG than for standard ECoG (**Figure 2a**, $10.30 \pm 10.40 \text{ FR/min}$ vs. $2.62 \pm 2.23 \text{ FR/min}$, $p = 0.0360$, Wilcoxon rank sum test).

3.6 FR rate and surgery outcome

With standard ECoG, we found FR in 5 of 12 cases in pre-resection recordings but only in 1 of 14 cases in post-resection recordings. With hd-ECoG, we found FR in all 8 cases in pre-resection recordings and in 1 of 8 cases with post-resection hd-ECoG. Taking all standard ECoG and hd-ECoG cases together, all three patients with residual FR in post-resection recordings suffered from recurrent seizures (ILAE > 1, PPV = 100%).

In post-resection recordings, the maximum FR rate in standard ECoG decreased in 4 cases and increased in 1 (seizure recurrence, ILAE 5) of 5 cases with FR in pre- or post-resection recordings. All 8 hd-ECoG cases had FR in pre- or post-resection recordings. Maximum FR rate decreased in all 8 cases, 7 of which achieved seizure freedom (ILAE 1).

For the secondary endpoint of our study, we identified residual FR in post-resection recordings of standard ECoG and hd-ECoG. The predictive power of residual FR for seizure outcome is shown in **Table 2**. There were no cases with residual FR and seizure freedom (FP=0), neither for standard ECoG nor for hd-ECoG, leading to a PPV and a specificity of 100%. For standard ECoG, NPV was 54% (FN=6) while for hd-ECoG NPV was 100%, since the only patient with seizure recurrence had residual FR (FN=0). Overall accuracy of seizure outcome prediction was 73% (CI [50 89%]) for all cases, 57% (CI [29 82%]) for standard ECoG, and 100% (CI [63 100%]) for hd-ECoG.

4 Discussion

4.1 Hd-ECoG improves FR detection

In this study, we performed intraoperative ECoG with high-density subdural electrodes and compared this new approach with ECoG performed with standard subdural electrodes. Regarding our primary endpoint, hd-ECoG improved FR detection of clinically relevant FR. Regarding our secondary endpoint, the occurrence of residual FR predicted seizure recurrence. This is in agreement with previous studies showing that incomplete resection of cortical tissue generating FR correlates with seizure recurrence (Akiyama et al., 2011, Fedele et al., 2017b, Haegelen et al., 2013, van 't Klooster et al., 2015b, van 't Klooster et al., 2017, van Klink et al., 2014, Wu et al., 2010). Interestingly, the higher rate of residual FR in post-resection hd-ECoG improved the prediction of seizure recurrence (100% vs. 50%) compared to

standard ECoG, although this finding did not reach statistical significance in our study.

4.2 Detecting small FR with dense spatial sampling

FR generators are very small and the spatial attenuation of the signal is high (Burnos et al., 2016, Jiruska et al., 2017, von Ellenrieder et al., 2014). The main advantage of hd-ECoG arises from denser spatial sampling compared to standard ECoG. The effect of this denser spatial sampling of hd-ECoG is two-fold. First, the smaller inter-electrode distance for hd-ECoG increases the probability of measuring from the point of maximal intensity of the FR generator over the sampled tissue. Therefore, the dense spatial sampling increases the probability of detecting an FR. Additionally, the electrode contacts are more likely to be closer to the generator, which leads to a higher FR amplitude in the recording. Furthermore, unlike standard strip electrodes, the grid electrodes of hd-ECoG cover the cortical tissue in the two dimensions of the grid, thereby increasing the chance of fully covering the epileptogenic zone and detecting HFO. Second, the bipolar channel over a smaller patch of cortex (5 vs. 10 mm) detects a lower amount of additional signal contributions, thereby decreasing the noise level. This enhanced signal-to-noise ratio facilitates the detection of a higher number of clinically relevant FR (Fedele et al., 2017b). However, the smaller contact size also results in higher impedance and consequently higher noise level, which in turn reduces the signal-to-noise ratio. The relative importance of these competing factors needed experimental quantification: our study suggests that denser spatial sampling improves FR detection. Detecting more FR reduces the number of falsely predicted cases of seizure freedom and thereby improves seizure outcome prediction.

4.3 Limitations

Regarding the comparison of hd-ECoG to standard ECoG, our primary endpoint, our study design did not permit a direct comparison between electrode types. First, the different electrode types were not placed on the same brain tissue. Second, the hd-ECoG electrode covered a larger surface than a standard strip electrode. Therefore, the improved FR detection in hd-ECoG could be a consequence of either the wider coverage or denser spatial sampling or both.

Regarding the seizure outcome prediction by residual FR in the individual patient, our secondary endpoint, limitations are posed by the overall small sample size and by the

unbalanced seizure outcome between the subgroups that underwent standard ECoG and hd-ECoG guided surgery (van 't Klooster et al., 2015a). Even though we observed a considerable increase in the prediction accuracy from 57% for standard ECoG to 100% for hd-ECoG, this observation did not reach statistical significance in our study.

Another constraint is the small extent of craniotomy performed in our institution, which limits the electrode size that can be placed and thus the brain tissue coverage. In some cases, spatial constraints precluded the use of hd-ECoG and thus required the use of standard ECoG. However, the use of hd-ECoG or standard ECoG was not related to the complexity of the cases or to any other reasons that could be responsible for the difference in FR occurrence.

In the presence of these limitations, hd-ECoG optimized the detection of clinically relevant FR.

4.4 Future developments of hd-ECoG for clinical application

The intraoperative hd-ECoG provided a more reliable intraoperative assessment of tissue epileptogenicity. However, in some cases, a more extensive coverage of the potentially epileptogenic tissue would have been desirable. To increase coverage combined with dense spatial sampling, scalable, flexible and non-invasive electrode designs with large channel numbers have been proposed (Khodagholy et al., 2016, Viventi et al., 2011). Still, the impedance of the electrode contacts should remain sufficiently low for optimal FR detection. We expect these developments to further improve the detection of small amplitude fast components in the ECoG.

5 Conclusions

We found that hd-ECoG, when compared to standard-ECoG, 1) increased the number of detected FR and 2) improved the prediction of seizure outcome based on FR. The main advantage of hd-ECoG over standard ECoG is that it enables denser spatial sampling of FR generators. Hd-ECoG may thereby advance seizure freedom after epilepsy surgery.

6 Acknowledgements

We thank Dr. P. Hilfiker, Schweizerische Epilepsie-Klinik, for his assistance in recordings. We acknowledge grants awarded by the Swiss National Science Foundation (SNSF 320030_176222 to J. S.), Mach-Gaensslen Stiftung (to J.S.),

Stiftung für wissenschaftliche Forschung an der Universität Zürich (to J.S.) and by
Forschungskredit der Universität Zürich (to T.F.). The funders had no role in the
design or analysis of the study.

Author contributions

T.F., E.B., G.R., and J.S. designed the experiments. G.R., J.S., T.F., and E.B.
performed recordings. E.B., T.F., M.S. analyzed the data. G.R. and K.K. provided
patient care. N.K. performed surgery. E.B., G.R., T.F., and J.S. wrote the manuscript.
All authors reviewed the final version of the manuscript.

Competing interests

All authors declare that they have no competing interests.

Data availability

The code is freely available at the GitHub repository
([https://github.com/ZurichNCH/Automatic-High-Frequency-Oscillation-](https://github.com/ZurichNCH/Automatic-High-Frequency-Oscillation-Detector)
Detector). The ECoG data and FR markings are freely available at [https://gin.g-](https://gin.g-node.org/USZ_NCH/Intraoperative_ECoG_HFO)
[node.org/USZ_NCH/Intraoperative_ECoG_HFO](https://gin.g-node.org/USZ_NCH/Intraoperative_ECoG_HFO).

7 References

- Akiyama T, McCoy B, Go CY, Ochi A, Elliott IM, Akiyama M, et al. Focal resection of
fast ripples on extraoperative intracranial EEG improves seizure outcome in
pediatric epilepsy. *Epilepsia* 2011;52(10):1802-11.
- Burnos S, Fedele T, Schmid O, Krakenbuhl N, Sarnthein J. Detectability of the
somatosensory evoked high frequency oscillation (HFO) co-recorded by scalp
EEG and ECoG under propofol. *Neuroimage Clin* 2016;10:318-25.
- Burnos S, Hilfiker P, Surucu O, Scholkmann F, Krakenbuhl N, Grunwald T, et al.
Human intracranial high frequency oscillations (HFOs) detected by automatic
time-frequency analysis. *PLoS One* 2014;9(4):e94381.
- Fedele T, Burnos S, Boran E, Krakenbuhl N, Hilfiker P, Grunwald T, et al. Resection
of high frequency oscillations predicts seizure outcome in the individual patient.
Sci Rep 2017a;7(1):13836.
- Fedele T, Ramantani G, Burnos S, Hilfiker P, Curio G, Grunwald T, et al. Prediction
of seizure outcome improved by fast ripples detected in low-noise intraoperative
corticogram. *Clin Neurophysiol* 2017b;128(7):1220-6.
- Fedele T, Ramantani G, Sarnthein J. High frequency oscillations as markers of
epileptogenic tissue - End of the party? *Clin Neurophysiol* 2019;130(5):624-6.
- Fedele T, van 't Klooster M, Burnos S, Zweiphenning W, van Klink N, Leijten F, et al.
Automatic detection of high frequency oscillations during epilepsy surgery predicts
seizure outcome. *Clin Neurophysiol* 2016;127(9):3066-74.
- Frauscher B, Bartolomei F, Kobayashi K, Cimbalnik J, van 't Klooster MA, Rampp S,
et al. High-frequency oscillations: The state of clinical research. *Epilepsia*
2017;58(8):1316-29.

Grewal SS, Alvi MA, Perkins WJ, Cascino GD, Britton JW, Burkholder DB, et al. Reassessing the impact of intraoperative electrocorticography on postoperative outcome of patients undergoing standard temporal lobectomy for MRI-negative temporal lobe epilepsy. *J Neurosurg* 2019;1-10.

Haegelen C, Perucca P, Chatillon CE, Andrade-Valenca L, Zelman R, Jacobs J, et al. High-frequency oscillations, extent of surgical resection, and surgical outcome in drug-resistant focal epilepsy. *Epilepsia* 2013;54(5):848-57.

Jette N, Reid AY, Wiebe S. Surgical management of epilepsy. *CMAJ* 2014;186(13):997-1004.

Jiruska P, Alvarado-Rojas C, Schevon CA, Staba R, Stacey W, Wendling F, et al. Update on the mechanisms and roles of high-frequency oscillations in seizures and epileptic disorders. *Epilepsia* 2017;58(8):1330-9.

Khodagholy D, Gelinas JN, Zhao Z, Yeh M, Long M, Greenlee JD, et al. Organic electronics for high-resolution electrocorticography of the human brain. *Sci Adv* 2016;2(11):e1601027.

Ryvlin P, Cross JH, Rheims S. Epilepsy surgery in children and adults. *Lancet Neurol* 2014;13(11):1114-26.

Thomschewski A, Hincapie AS, Frauscher B. Localization of the Epileptogenic Zone Using High Frequency Oscillations. *Front Neurol* 2019;10(94):94.

van 't Klooster MA, Leijten FS, Huiskamp G, Ronner HE, Baayen JC, van Rijen PC, et al. High frequency oscillations in the intra-operative ECoG to guide epilepsy surgery ("The HFO Trial"): study protocol for a randomized controlled trial. *Trials* 2015a;16(1):422.

van 't Klooster MA, van Klink NE, Leijten FS, Zelman R, Gebbink TA, Gosselaar PH, et al. Residual fast ripples in the intraoperative corticogram predict epilepsy surgery outcome. *Neurology* 2015b;85(2):120-8.

van 't Klooster MA, van Klink NEC, Zweiphenning W, Leijten FSS, Zelman R, Ferrier CH, et al. Tailoring epilepsy surgery with fast ripples in the intraoperative electrocorticogram. *Ann Neurol* 2017;81(5):664-76.

van Klink NEC, Van't Klooster MA, Zelman R, Leijten FSS, Ferrier CH, Braun KPJ, et al. High frequency oscillations in intra-operative electrocorticography before and after epilepsy surgery. *Clin Neurophysiol* 2014;125(11):2212-9.

Viventi J, Kim DH, Vigeland L, Frechette ES, Blanco JA, Kim YS, et al. Flexible, foldable, actively multiplexed, high-density electrode array for mapping brain activity in vivo. *Nat Neurosci* 2011;14(12):1599-605.

von Ellenrieder N, Beltrachini L, Perucca P, Gotman J. Size of cortical generators of epileptic interictal events and visibility on scalp EEG. *Neuroimage* 2014;94:47-54.

Wu JY, Sankar R, Lerner JT, Matsumoto JH, Vinters HV, Mathern GW. Removing interictal fast ripples on electrocorticography linked with seizure freedom in children. *Neurology* 2010;75(19):1686-94.

Zijlmans M, Jacobs J, Zelman R, Dubeau F, Gotman J. High-frequency oscillations mirror disease activity in patients with epilepsy. *Neurology* 2009a;72(11):979-86.

Zijlmans M, Jacobs J, Zelman R, Dubeau F, Gotman J. High frequency oscillations and seizure frequency in patients with focal epilepsy. *Epilepsy Res* 2009b;85(2-3):287-92.

Zijlmans M, Worrell GA, Dumpelmann M, Stieglitz T, Barborica A, Heers M, et al. How to record high-frequency oscillations in epilepsy: A practical guideline. *Epilepsia* 2017;58(8):1305-15.

8 Table and figure captions

8.1 Table 1. Seizure outcome and pre- and post-resection FR rate.

Abbreviations: FCD = focal cortical dysplasia; DNET = dysembryoplastic neuroepithelial tumors; ODG = oligodendroglioma; L = left; R = right. TP = True Positive; TN = True Negative; FP = False Positive; FN = False Negative.

8.2 Table 2. Prediction of surgery outcome for standard ECoG and hd-ECoG.

Hd-ECoG improved seizure outcome prediction over standard ECoG. Abbreviations: TP = True Positive; TN = True Negative; FP = False Positive; FN = False Negative; PPV = Positive predictive value; NPV = Negative predictive value; Sens = Sensitivity; Spec = Specificity; ACC = Accuracy; CI = 95% confidence interval.

	standard ECoG	high-density ECoG	all
PPV = $TP/(TP+FP)$ [%]	100	100	100
NPV = $TN/(TN+FN)$ [%]	54	100	70
Sens = $TP/(TP+FN)$ [%]	14	100	25
Spec = $TN/(TN+FP)$ [%]	100	100	100
ACC = $(TP+TN)/(P+N)$ [%]	57	100	73
ACC upper CI [%]	82	100	89
ACC lower CI [%]	29	63	50

8.3 Figure 1. FR in pre-resection standard ECoG and hd-ECoG.

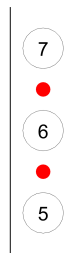
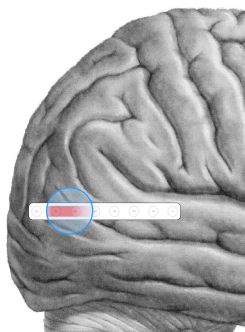
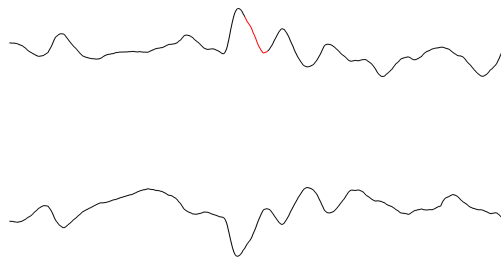
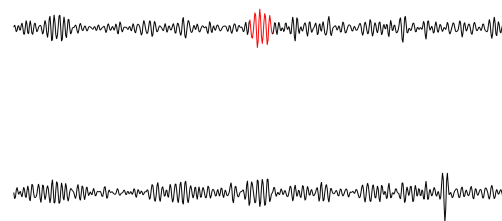
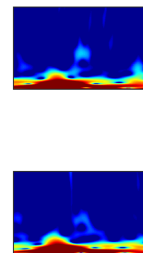
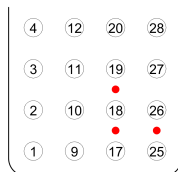
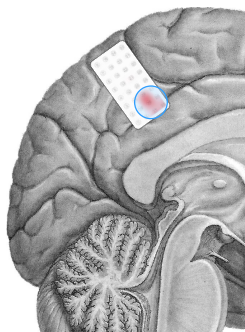
a) Patient 13 underwent a right parietal resection (blue circle) for cavernoma-associated refractory epilepsy. In the pre-resection recording, a standard ECoG was placed across the planned resection area in the lateral convexity. The inset shows the electrode with the channels of the bipolar montage where we recorded the traces in panels b, c, d. The upper trace shows a typical FR (red line) in (b) full-band ECoG and (c) ECoG filtered in the FR band (250-500 Hz), where the FR had a maximum amplitude of 2.8 μ V. The lower trace shows the adjacent bipolar channel, where no FR were detected. (d) In the Stockwell time-frequency representation of the signal, the FR stands out as a separate blob. Although the tissue under the channels with high FR rate was fully resected and no FR were detected in post-resection ECoG, the patient had no improvement in seizure frequency after surgery (ILAE 5), therefore his case was classified as False Negative (FN). e) Patient 1 underwent a left parietal resection (blue circle) for glioneuronal tumor-associated refractory epilepsy. In the pre-resection recording, an hd-ECoG electrode was placed across the planned resection area in the interhemispheric space. The upper trace shows a typical FR (red line) in (f) full-band ECoG and (g) filtered ECoG in the FR band (250-500 Hz), where the FR had a maximum amplitude of 15.7 μ V. The center trace shows an adjacent bipolar channel, where the same FR was detected. The lower trace shows another adjacent bipolar channel, where no FR was detected. In panels c and g, the spacing between traces is proportional to the spacing between contacts (10 mm for standard ECoG, 5 mm for hd-ECoG). (h) In the Stockwell time-frequency representation of the signal, the FR stands out as a separate blob. The tissue under the channels with high FR rate was fully resected. No FR were detected in post-resection ECoG and the patient remained seizure free (ILAE 1) at last follow-up of almost 3 years, therefore his case was classified as True Negative (TN).

8.4 Figure 2. FR rate is higher in hd-ECoG than in standard ECoG.

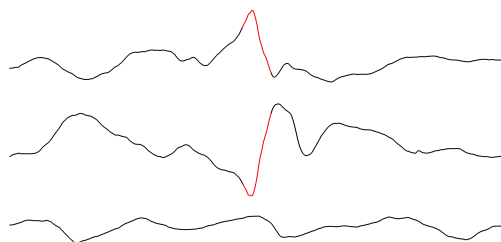
a) The average FR rate across hd-ECoG recordings was significantly higher than across standard ECoG recordings (10.30 ± 10.40 FR/min vs. 2.62 ± 2.23 FR/min, $p = 0.0360$, Wilcoxon rank sum test) $*p < 0.05$.

b) The maximum FR amplitude across hd-ECoG recordings seemed higher than across standard ECoG recordings (15.29 ± 13.65 μ V vs. 10.74 ± 12.85 μ V, n.s.), but this finding did not reach statistical significance.

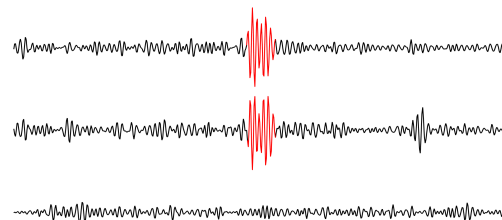
Patient	Age, gender	Etiology	Resection area	Follow-up period	Type of electrodes	ECoG duration		Max FR rate		Outcome	Prediction
				[months]		Pre	Post	Pre	Post		
						[min]		[FR/min]		[ILAE scale]	
1	15, f	DNET (WHO I)	L medial parietal	33	4x8 hd-ECoG	8.3	2.0	6.0	< 1	1	TN
2	7, f	FCD 2b	L dorsal medial prefrontal	24	4x8 hd-ECoG	4.9	3.3	3.5	< 1	1	TN
3	17, m	Sturge Weber syndrome	L lateral occipital	30	4x8 hd-ECoG	1.5	2.7	2.0	< 1	1	TN
4	22, m	ganglioglioma (WHO I)	R posterior fusiform gyrus (occipital)	18	4x8 hd-ECoG	1.5	3.9	7.9	< 1	1	TN
5	20, f	FCD 2a	R posterior temporal	13	4x8 hd-ECoG	5.0	2.3	13.2	< 1	1	TN
6	3, f	Sturge Weber syndrome	R lateral posterior temporal & lateral occipital	20	4x8 hd-ECoG	3.9	2.0	31.7	4.6	3	TP
7	34, m	astrocytoma (WHO II)	R posterior middle frontal gyrus	29	2x14 hd-ECoG	3.9	5.6	1.3	< 1	1	TN
8	23, f	FCD 2a	R posterior cingulate gyrus, posterior hippocampus	12	4x8 hd-ECoG	3.5	3.4	22.4	< 1	1	TN
9	1, m	FCD 2a	R dorsal lateral prefrontal	43	1x4 standard ECoG	4.9	3.6	1.8	< 1	1	TN
10	15, f	Sturge Weber syndrome	L lateral parieto-occipital & medial temporal	30	1x6 standard ECoG	3.4	2.4	< 1	< 1	3	FN
11	36, f	ependymoma (WHO II)	R posterior angular gyrus	28	1x6 standard ECoG	3.8	5.5	< 1	< 1	1	TN
12	38, m	anaplastic astrocytoma (WHO III)	R insulo opercular	14	1x6 standard ECoG	2.0	2.4	< 1	< 1	1	TN
13	42, f	cavernoma	R angular gyrus	29	1x8 standard ECoG	2.6	2.8	1.2	< 1	5	FN
14	7, f	FCD 2b	L dorsal medial prefrontal	16	1x6 standard ECoG	2.8	3.4	1.8	< 1	1	TN
15	17, m	FCD 3	L lateral posterior temporal & lateral occipital	35	1x6 standard ECoG	n.a.	6.0	n.a.	< 1	5	FN
16	67, f	ODG (WHO II)	R occipital	31	1x4 standard ECoG	1.5	2.5	< 1	< 1	1	TN
17	3, f	FCD 2a	R medial/lateral anterior temporal	36	1x6 standard ECoG	n.a.	3.8	n.a.	< 1	3	FN
18	4, m	FCD 1a	L medial/lateral anterior temporal	13	2x8 standard ECoG	3.3	5.2	1.2	2.7	5	TP
19	17, m	hippocampal sclerosis, gliosis	R medial/lateral temporal	40	2x8 standard ECoG	3.0	3.0	< 1	< 1	5	FN
20	4, m	FCD 1c	R medial/lateral anterior temporal	38	1x4 standard ECoG	3.7	3.3	7.0	< 1	1	TN
21	41, m	cavernoma	L supramarginal gyrus (parietal)	35	2x8 standard ECoG	1.1	4.1	< 1	< 1	5	FN
22	5, f	fibrillary astrocytoma (WHO II)	R medial/lateral parietal	40	1x4 standard ECoG	10.0	4.7	< 1	< 1	1	TN

a**b****c****d****e**

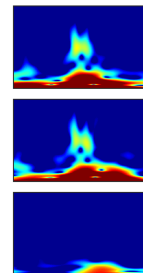
10 mm

f

700 μV
50 ms

g

10 μV
50 ms

h

500 Hz
50 ms

